Received: 12 March 2022 | Revised: 8 June 2023 | Accepted: 9 June 2023

DOI: 10.1002/joc.8161

RESEARCH ARTICLE

International Journal of Climatology RMetS

Stochastic disaggregation of seasonal precipitation forecasts of the West African Regional Climate Outlook Forum

Mandela Coovi Mahuwètin Houngnibo[1,2,3] | **Abdou Ali**[1] | **Alhassane Agali**[1] | **Moussa Waongo**[1] | **Agnidé Emmanuel Lawin**[3] | **Jean-Martial Cohard**[4]

[1]Department of Information and Research, Regional Center AGRHYMET, Niamey, Niger

[2]Section Studies and Training, Agence Nationale de la Météorologie du BENIN (METEO BENIN), Cotonou, Benin

[3]Laboratoire d'Hydrologie Appliquée, Institut National de l'Eau (University of Abomey-Calavi), Abomey-Calavi, Benin

[4]Université Grenoble Alpes, CNRS, IRD, Institut des Géosciences de l'Environnement (IGE), UMR 5001, Grenoble, France

Correspondence
Mandela Coovi Mahuwètin Houngnibo, Section Studies and Training, METEO BENIN, Cotonou 229, Benin.
Email: hmandelahmadiba@gmail.com

Funding information
Accelerating Impacts of CGIAR Climate Research for Africa (AICCRA) project, Grant/Award Number: P173398

Abstract

Seasonal rainfall forecasts from the West African Regional Climate Outlook Forum (RCOF) are essential for adapting to climate variability. However, their temporal aggregated nature is a strong limitation, especially when used with impact models requiring daily resolution, such as hydrological or crop models. To address this issue, this study proposes a temporal disaggregation method for these forecasts using in situ data from two districts (Kandi and Parakou) in northern Benin, spanning from 1971 to 2020. A resampling technique was used to construct a daily historical record that aligns with seasonal rainfall forecasts. Three stochastic disaggregation models for rainfall (SRGs) were developed, including two parametric models (SRG1 and SRG2) and one semiparametric (SRG3). Their parameters were estimated from the resampled record to generate daily synthetic data replicating the forecasts. Evaluation of the SRGs revealed that SRG2, which combined a first-order Markov chain with a mixed exponential distribution, performs well in simulating various characteristics of the rainy season, including dry spells, wet spells and daily precipitations. Furthermore, SRG2 maintained the trends of the initial forecasts and outperformed SRG1 and SRG3, as confirmed by the chi-square test. Indeed, a good agreement was observed between the probabilities of the initial prediction and those calculated from the temporal disaggregation with the SRG2 method. Also, for the forecasts expressed by probabilities 15–35–50 and 20–50–30, the cumulative distribution function curves (CDF) of the SRGs exhibited appropriate shifts compared to climatology. These forecasts were specific to the Kandi area in 2008 and 2003, respectively, during the West African RCOFs. Although this study focused specifically on the Kandi and Parakou districts, the temporal disaggregation methodology used can be applied to other locations within West Africa or other RCOFs worldwide. This study offers valuable guidance for generating sector-specific seasonal forecasts for the West African region.

KEYWORDS

Regional Climate Outlook Forum, seasonal rainfall forecasts, stochastic disaggregation models, West Africa

1 | INTRODUCTION

Seasonal rainfall forecasts are important for adapting to climate variability, especially in regions with high inter-annual rainfall variability (Hansen et al., 2011; Sultan et al., 2010). In recent decades, forecasting capabilities have improved due to research showing that seasonal rainfall variability is strongly related to large-scale interactions between the oceans and the atmosphere (Fontaine et al., 2011; Parhi et al., 2016). Seasonal forecasts are produced routinely at several operational weather centres around the world. World meteorological centres such as the European Center for Medium-Range Weather Forecasts (ECMWF) and the National Oceanic and Atmospheric Administration (NOAA) run coupled ocean-atmospheric circulation models (AOGCMs) with resolutions ranging from 0.25° to 2° to produce seasonal climate forecasts. Some of these models provide probabilistic outputs, along with daily weather parameters for the upcoming season (Baigorria et al., 2008; Challinor et al., 2003). However, the daily series derived from these AOGCMs exhibit certain limitations (Ali et al., 2006). They use to overestimate the number of rainy events, resulting in an unrealistic distribution of dry and wet spells, and they underestimate rainfall amounts. Also, the coarse resolution of AOGCMs' grid cells often fails to accurately depict climate zone boundaries or areas of specific interest.

In West Africa, the African Center for Meteorological Applications for Development (ACMAD) and the Regional Center AGRHYMET (CRA) act as regional coordinators for seasonal climate forecasts. They provide support to national meteorological and hydrological services (NMHS) in the region through the organization of regional climate outlook forums (RCOFs). Previously known as seasonal forecasts in West Africa (PRESAO), these forums have been subdivided into two categories: seasonal forecasts for the Sudano-Sahelian region of West Africa (PRESASS) and seasonal forecasts for countries along the Gulf of Guinea (PRESAGG). This subdivision takes into account the distinct rainfall regimes between the Gulf of Guinea and the Sudano-Sahelian regions of West Africa. The PRESAGG RCOF typically takes place in the second half of February and provides seasonal rainfall forecasts (ACMAD, 2022a) for the early monsoon phase (March–May, April–June). On the other hand, PRESASS RCOF is held late in April and provides seasonal rainfall forecasts (ACMAD, 2022b) for the peak of the monsoon (June–August, July–September). The forecasting procedure is a mixture of objective and subjective approaches (for more details, see Bliefernicht et al., 2019). First, NMHS performs country-scale seasonal rainfall forecasts using statistical techniques (objectives or automated approaches), such as canonical correlation analysis, principal component regression, or multiple linear regression, implemented in the climate predictability tool (Mason et al., 2022). These techniques establish statistical relationships between the forecast variables (explained variables) and the predictors, such as the sea surface temperatures output by AOGCMs (Chidzambwa & Mason, 2008; Kumar et al., 2020). Second, subjective or manual techniques, based on the expertise of climatologists from NHMS, CRA, ACMAD and other experts (from world meteorological centres), are used alongside statistical methods to carry out the regional harmonization (Bliefernicht et al., 2019). These techniques involve analysing the main climate driver fields of West Africa as predicted by AOGCMs or other data sources. Based on consensus, the regions where precipitation anomalies are expected are delineated, and the probabilities of the forecast are assigned to the categories (terciles) above-average, average and below-average (see the example in Figure 1). These terciles are defined based on the most recent 30-year record, updated every 10 years. Thus, the seasonal forecast for the year 2022 considered the terciles computed for the period 1991–2020. Finally, they communicated and disseminated precipitation forecasts to end-users during a broadcast press conference directly after the RCOF meteorological experts' meeting. These forecasts are essential for various sectors, especially agriculture. Sultan et al. (2013) and Roudier et al. (2011) showed that despite the uncertainties associated with these forecasts, farmers could benefit from them in terms of increased income and reduced risks by implementing the related advice and recommendations. Besides, some studies have evaluated the West African RCOFs seasonal rainfall forecasts and shown that the forecasts have improved over time (Bliefernicht et al., 2019; Chidzambwa & Mason, 2008). These studies concluded that the forecasts are reliable for the above-average and below-average categories. However, some systematic errors have been reported, the most common being the tendency of experts to assign high probabilities to the average category due to risk aversion (Bliefernicht et al., 2019).

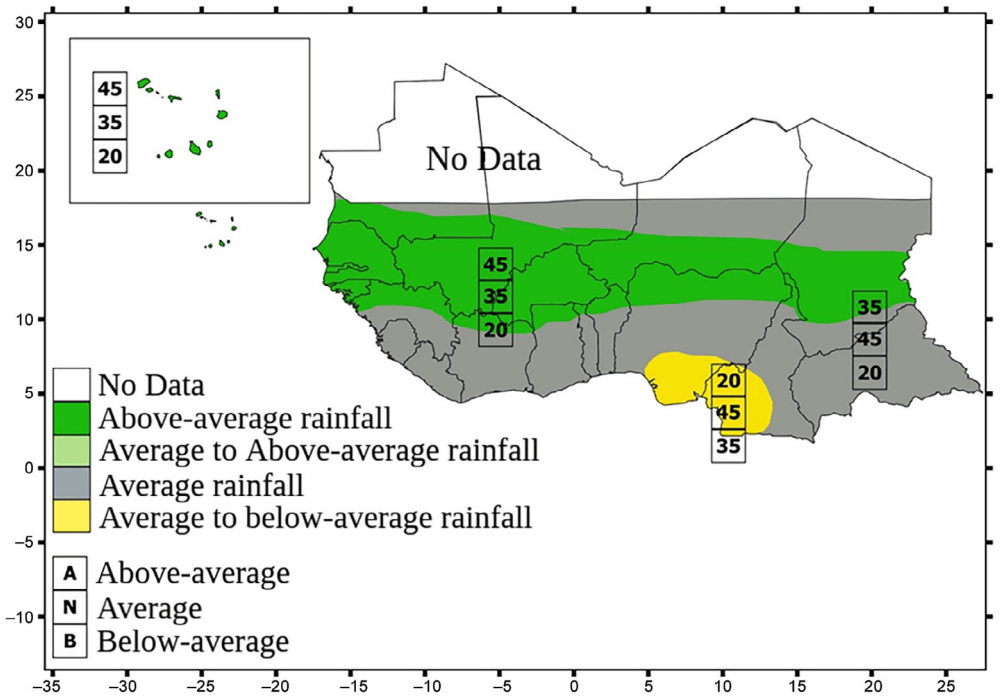

FIGURE 1 Seasonal rainfall forecast map for July–August–September 2022, issued in April 2022 (adapted map from CRA) [Colour figure can be viewed at wileyonlinelibrary.com]

Unlike global climate centres, seasonal rainfall forecasts in West Africa do not provide a daily precipitation series for the upcoming season. The importance of daily meteorological series for the upcoming season lies in their use as input for models, including crop and hydrological models, to assess the impacts of the expected season on water resources and crops (Baigorria et al., 2008; Wilks, 2002). This enables the formulation of appropriate adaptation options for end-users, such as optimal sowing dates, efficient water management, fertilizer usage and enhanced water and soil conservation techniques. Crop models, for example, are used as decision-support tools, predicting phenology, growth, yield and, in some cases, crop quality based on different crop management practices and climate (Equation (1)). These models primarily simulate plant development and growth, relying predominantly on daily data as input variables. Most downstream applications of the seasonal rainfall forecasts from the West African RCOFs require temporal disaggregation. However, no studies have been conducted to disaggregate these forecasts into finer temporal scales since the establishment of the West African RCOFs.

This study is part of this framework and uses a stochastic approach. It aims to disaggregate the seasonal rainfall products of the West African RCOF on a daily time scale. It can be used to develop specific seasonal forecasts, such as seasonal forecasts of crop yield, seasonal forecasts of the phenological stage and seasonal forecasts of stream flow, by integrating disaggregated series in these impact models.

This paper is divided into four sections. The section 1 focuses on the methodology employed and the areas selected for applying the methods. The results are presented in section 2, while in section 3, we discuss the results and highlight some limitations. Finally, in conclusion, we summarize the key findings of this study and present some perspectives.

2 | METHODOLOGY

Temporal disaggregation of seasonal forecasts consists in reproducing seasonal forecasts on a finer temporal scale. This process does not enhance the initial forecasts, which are already deemed reliable enough to meet end-users needs. Some authors have used stochastic weather generators (SWGs) to perform this temporal disaggregation. The parameters of these SWGs are based on historical data that align with the seasonal forecasts (Apipattanavis et al., 2007; Ghosh et al., 2014; Han et al., 2017; Han & Ines, 2017; Kim et al., 2015; Wilks, 2002). SWGs are stochastic methods specifically designed to simulate synthetic time series of meteorological variables, theoretically of infinite length, for a specific location. These simulations are based on the statistical properties of observed weather patterns at that particular location (Peleg et al., 2017; Wilks & Wilby, 1999). These methods aim to generate time series that accurately replicate the observations by considering essential characteristics such as means,

variances, frequencies and extremes. The literature provides various types of stochastic weather generators (SWGs), which can be classified into two main approaches: statistical and a combination of statistical and process-based methods (Peleg et al., 2017). Our study focuses on the statistical SWGs, which can be parametric, nonparametric or semiparametric. Parametric SWGs assume a specific distribution for the observed historical rainfall series, while nonparametric SWGs do not make such assumptions. Semiparametric models combine elements of both parametric and nonparametric approaches.

Wilks (2002) presented a method for conditioning parametric SWGs using probabilistic seasonal climate forecasts. This method was applied using the New York State rainfall and temperature station network to estimate SWG parameters by resampling the historical series to align with the seasonal forecasts for the area (see Briggs & Wilks, 1996). Kim et al. (2015) employed a similar approach with an SWG based on a generalized linear model. The weighted resampling technique of Briggs and Wilks (1996) and Ines (2013) was applied to nonparametric and semiparametric SWG to condition synthetic weather series by seasonal climate forecasts. For example, Apipattanavis et al. (2007, 2010) modified their semiparametric SWG based on the *k*-nearest neighbour approach to select neighbours randomly not from the raw historical series but from a resampling of historical climate data consistent with the outputs of seasonal forecasts. Similarly, to disaggregate the seasonal rainfall forecasts of the West African RCOF, we developed three models called stochastic disaggregation models for rainfall (SRG), which differ from SWGs as they concern only the rainfall. The three developed SRGs include two parametric and one semiparametric in order to choose the best-performing one. Using the Briggs and Wilks (1996) methodology, we resampled our historical rainfall time series and estimated the parameters of the three models from these series.

2.1 | Construction of historical records consistent with seasonal rainfall forecasts

The methodology for a forecast expressed in terms of probabilities $p_B - p_N - p_A$ corresponding to below-average (p_B), average (p_N) and above-average (p_A), respectively (Figure 1) is summarized in four steps according to Wilks (2002) and Briggs and Wilks (1996).

Step 1: The first step involves calculating the cumulative seasonal rainfall (R_{SP}) for the target season, such as July–August–September, from the historical rainfall time series for all years.

Step 2: Next, the terciles of the cumulative seasonal rainfall are computed. These terciles, denoted as $Q_{1/3}$ and $Q_{2/3}$, divide the sorted statistical series into three equal groups, each containing 33% of the data. These statistics were calculated using the type 5 definition from Hyndman and Fan (1996), which is widely accepted among hydrologists and builds upon the research conducted by Hazen (1914).

Step 3: Each year in the historical series is then classified into one of three categories: below-average ($R_{SP}<Q_{1/3}$), average ($Q_{1/3}<R_{SP}<Q_{2/3}$), or above-average ($R_{SP}>Q_{2/3}$), based on the total rainfall for the considered season. Thus, the historical rainfall series consists of N years, where $N=N_A+N_B+N_N$, with N_B years categorized as below-average rainfall, N_N years as average rainfall and N_A years as above-average rainfall.

Step 4: The resampled dataset (or the built rainfall times series) is generated by drawing a sample of size L (where $L=1000$) with replacement from the historical rainfall time series, considering the probabilities (p_A, p_N, p_B) associated with each category. The resulting climate series comprises subsets of sizes p_BL, p_NL and p_AL, obtained by drawing with replacement from the N_B years with below-average rainfall, N_N years with average rainfall and N_A years with above-average rainfall, respectively.

Wilks (2002) demonstrated that some SRG parameters could be estimated from the built rainfall times series. The author explained that these parameters can be considered as simple seasonal statistics and that their expected values can be estimated from the built rainfall times series. Specifically, considering seasonal statistics denoted as X and $x_i^{(B)}$, $x_i^{(N)}$ and $x_i^{(A)}$ representing the statistics of interest in the ith below-average, average and above-average years, respectively. The expected value of X can be calculated using Equation (1),

$$E(X)=\lim_{L\to\infty}\frac{1}{L}\left[\sum_{i=1}^{N_B}\frac{P_BL}{N_B}x_i(B)+\sum_{i=1}^{N_N}\frac{P_NL}{N_N}x_i(N)+\sum_{i=1}^{N_A}\frac{P_AL}{N_A}x_i(A)\right]. \quad (1)$$

Thus, the forecast-conditional value of X is a weighted sum of its mean in the below-average, average and above-average years, with the weights equal to the forecast probabilities for each of the three categories.

2.2 | Stochastic disaggregation models for rainfall

Three SRGs were developed, including two parametric models and one semiparametric model (Table 1). The

TABLE 1 Summary of the methods developed

Name of SRG	Type of SRG	Methods	Performance evaluation tests
SRG1	Parametric	Rainfall occurrence: first-order two-state Markov chain Rainfall amounts: Gamma distribution	Wilcoxon test Ho: means of SRGs and Obs are equal Ha: means of SRGs and Obs are different
SRG2	Parametric	Rainfall occurrence: First-order two-state Markov chain Rainfall amounts: mixed exponential distribution	Ansari-Bradley test Ho: SRGs and Obs are identical by dispersion Ha: SRGs and Obs differ by dispersion
SRG3	Semiparametric	Rainfall occurrence: First-order three-states Markov chain Rainfall amounts: Kernel density estimation	Kolmogorov–Smirnov test Ho: SRGs and Obs come from the same distribution Ha: SRGs and Obs do not come from the same distribution

Note: SRG means stochastic disaggregation models for rainfall.

parameters of these three SRGs were estimated from the built rainfall times series. This could enable the generation of synthetic daily data consistent with seasonal rainfall forecasts.

Parametric SRGs use the same model (first-order two-state Markov chain) to generate rainfall occurrences but differ in the model simulating precipitation amounts. Let $\{J_d : d=1,2,3,\ldots\}$ be a sequence of the daily occurrence of precipitation with $J_d=1$ or $J_d=0$, indicating that the day d was rainy (rainfall amount >0.1) or dry, respectively. It is accepted (Gabriel & Neumann, 1962; Katz, 1977) that this process is a first-order (the probabilities depend only on the state of the previous day) two states (rainy or dry) Markov chain. Jimoh and Webster (1996) found no significant difference between the performance of the first- and second-order Markov chains in their study in Nigeria. However, the first-order Markov chain outperformed the zero-order Markov chain. The first-order two-state Markov chain model is completely characterized by the transition probabilities: $P_{ij}=P_r\{J_d=j \mid J_{d-1}=i\}$, $i,j\in\{0,1\}$. Considering the theory of complementary probabilities, the two transition probabilities $P_{00}=1-P_{01}$ and $P_{10}=1-P_{11}$ are sufficient to define the process. We also define the unconditional probability of a rainy day π_1 and a dry day π_0 (Wilks, 2011) by Equation (2),

$$\pi_1=\frac{P_{01}}{1+P_{01}-P_{11}},\qquad \pi_0=1-\pi_1. \tag{2}$$

For the first parametric SRG (SRG1), a two-parameter Gamma distribution was used to estimate the precipitation amount on wet days. The density function of the Gamma distribution takes the following form (Equation (3)):

$$f(x)=\frac{(x/\beta)^{\alpha-1}\exp[(x/\beta)]}{\beta\Gamma(\alpha)}\quad \alpha,\beta>0, \tag{3}$$

where α is the shape parameter and β is the scale parameter. The second parametric SRG (SRG2) used the mixed exponential distribution to determine the amount of precipitation on wet days. This distribution is a probability mixture of 2 one-parameter exponential distributions, with the mixing parameter α controlling the use of either a larger (μ_1) or smaller (μ_2) exponential mean. The density function is in the form (Equation (4)),

$$f(x)=\frac{\alpha}{\mu_1}\exp\left(-\frac{x}{\mu_1}\right)+\frac{1-\alpha}{\mu_2}\exp\left(-\frac{x}{\mu_2}\right). \tag{4}$$

To simulate the occurrence of precipitation, a uniform random number (u) ranging from 0 to 1 was generated and compared to either P_{01} or P_{11} based on the previous day's condition (dry/wet). If the previous day was dry and $u\leq P_{01}$, the current day is considered wet. Conversely, if the previous day was dry and $u\geq P_{01}$, the current day is considered dry. The same comparison is performed when the previous day was wet but with u being compared to P_{11}. When the occurrence model simulates a wet day, a new uniform random number (u_1) is generated, and the precipitation amount for that rainy day is determined using the inverse of the cumulative distribution function (ICDF) of the exponential distribution for SRG1 and the mixed exponential distribution for SRG2 as follows: Amount$=f^{-1}(u_1)$. The initialization of the simulation, on the day $d=1$ for a given month, involves comparing u to the unconditional probability of a rainy day, π_1. If $u\leq\pi_1$, the first day is considered wet; otherwise, it is considered dry.

For the semiparametric SRG (SRG3), a first-order Markov chain with three-state (dry, wet and extremely

wet) is used to simulate the occurrence of precipitation. A day is considered dry ($J_d=0$) if the daily amount is less than or equal to 0.1 mm, extremely wet ($J_d=2$) if the daily amount is greater than or equal to the 80th percentile of the daily precipitation amount for the simulated month, and wet ($J_d=1$) otherwise. Six probabilities P_{01}, P_{02}, P_{11}, P_{12}, P_{21} and P_{22} are sufficient to define this Markov process. The unconditional probabilities for wet days (π_1), extremely wet days (π_2) and dry days (π_0) are given by the formulas (Equation (5)),

$$\begin{aligned}\pi_1&=\frac{P_{01}(1+P_{02}+P_{22})-P_{02}(P_{01}-P_{21})}{(1+P_{01}-P_{11})(1+P_{02}-P_{22})-(P_{01}-P_{21})(P_{02}-P_{12})},\\ \pi_2&=\frac{P_{02}-\pi_1(P_{02}-P_{12})}{1+P_{02}-P_{22}},\\ \pi_0&=1-(\pi_1+\pi_2).\end{aligned} \tag{5}$$

The precipitation amounts on wet and extremely wet days were estimated using the kernel method. Let $x_1,x_2,x_3,\ldots,x_n$ be a series of daily amounts on wet or extremely wet days. The probability density estimator using the kernel method is (Equation (6)),

$$\widehat{f}(x)=\frac{1}{nh}\sum_{i=1}^{n}K\left(\frac{x-x_i}{h}\right),\ x\in\mathbb{R}, \tag{6}$$

where x_i is the ith value of the series of size n, K is the kernel satisfying the conditions $K(x)>0$ and $\int_{-\infty}^{+\infty}K(x)dx=1$ and h is the bandwidth. A Gaussian kernel was chosen and h was estimated using Silverman's (1986) formula: $h\approx 1.06\widehat{\sigma}n^{-1/5}$, where $\widehat{\sigma}$ is the standard deviation of the series.

The simulation of precipitation occurrence at the initialization day ($d=1$ of the month) was carried out by comparing a uniform random number u with π_0 and $(\pi_0+\pi_1)$. The state on the first day is considered dry ($J_1=0$) if ($u<\pi_0$), wet ($J_1=1$) if $\pi_0<u<(\pi_0+\pi_1)$, and extremely wet ($J_1=2$) otherwise. The occurrences of the subsequent days are then determined by considering the state of the previous days and comparing the uniform random number u generated with the transition probabilities. For instance, if $J_1=0$, the state on the second day (J_2) is considered dry if $u<P_{00}$, wet if $P_{00}<u<(P_{00}+P_{01})$ and extremely wet otherwise. The process was iterated for each day until the last day of the month. The amounts of rain were generated using the inverse function of $\widehat{f}(x)$.

The forecast conditional values of the precipitation occurrence parameters (π_0, π_1, π_2, P_{01}, P_{11},...) were estimated using Equation (1). For example, π_0 was estimated each month as a function of p_B, p_A and the mean portion of dry days in below-normal $\overline{x}^{(B)}$, near-normal $\overline{x}^{(N)}$ and above-normal $\overline{x}^{(A)}$ years for that month as follows:

$$\pi_0=p_B\overline{X}^{(B)}+(1-p_B-p_A)\overline{X}^{(N)}+p_A\overline{X}^{(A)}. \tag{7}$$

The precipitation amount parameters cannot be estimated as a function of forecast probabilities such as occurrence parameters. Indeed, the parameters, α, μ, μ_1 and μ_2 are iteratively estimated using a maximum likelihood estimation approach, while $\widehat{f}(x)$ is estimated using the Gaussian kernel method. Consequently, these parameters are estimated from historical records consistent with the forecast as described above. They are separately estimated for each month of the target season and are considered constant for that month.

The evaluation of the three SRGs involved assessing their ability to capture certain statistics from historical rainfall time series (actual climatology). One hundred realizations, each of the same length as the historical rainfall record (50 years), were generated for the target season using each SRG. The evaluation focused on characteristics such as dry spells (consecutive days with rainfall amounts ≤0.1 mm), wet spells and cumulative daily rainfall for the season of interest. Nonparametric statistical tests were employed to examine the equality of means, variances and distributions between the observed and generated series. These tests included the Wilcoxon test for means, the Ansari-Bradley test for variances and the Kolmogorov–Smirnov test for distributions. A significance level of 5% was used, with a p-value less than 0.05 indicating rejection of the null hypothesis of equality and implying a significant difference. Conversely, for p-values exceeding 0.05, it is not possible to conclude the presence of a significant difference. Quantile–quantile graphs and probability density curves (PDF) were also generated to compare the distributions of the generated and observed series. A logarithmic transformation was applied to the daily rainfall amounts to enhance interpretation. The evaluation was conducted for the July–August–September (JAS) season, as it encompasses over 50% of the total annual rainfall in the study areas (Figure 3). Table 1 summarizes the SRG methods developed in this study.

2.3 | Seasonal rainfall forecast disaggregated

The consistency between the West African RCOF seasonal rainfall forecasts and those obtained from disaggregated forecasts was analysed. A total of 18 seasonal rainfall forecast formats ($P_B-P_N-P_A$) from the West African RCOF were disaggregated,

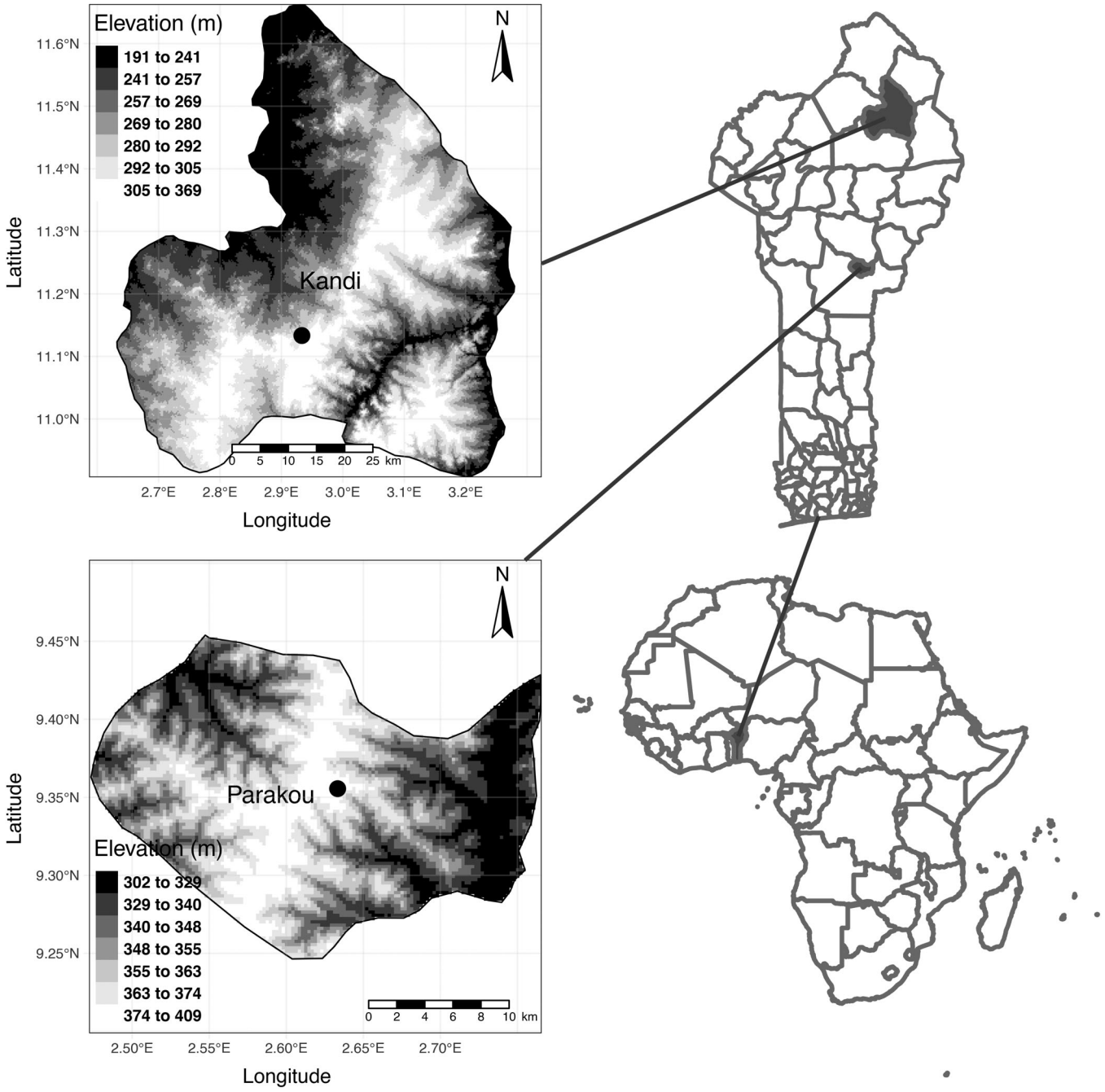

FIGURE 2 Topographic map of Kandi and Parakou, located within the Republic of Benin. The dots denote the location of the rain gauges used

including five above-average, five below-average, four average to above-average and four average to below-average forecasts. The disaggregation process involved conditionally generating 1000 simulations of 100 daily rainfall series for the JAS season for each forecast and station. The relative frequencies of seasonal cumulative rainfall falling below-average, average and above-average were determined from each simulation and compared with the initial probabilities of the disaggregated forecasts. To assess the agreement between the frequencies obtained and the initial forecast categories (P_B, P_N, P_A), a chi-square goodness-of-fit test was conducted at a significance level of 5% for each simulation.

Furthermore, forecasts expressed with probabilities 15–35–50 and 20–50–30 were also disaggregated. These forecasts were specific to the Kandi area in 2008 and 2003, respectively, during the West African RCOF. Cumulative distribution function curves were generated to compare the distributions of observed and simulated series. As the forecasts were issued for 2003 and 2008, the

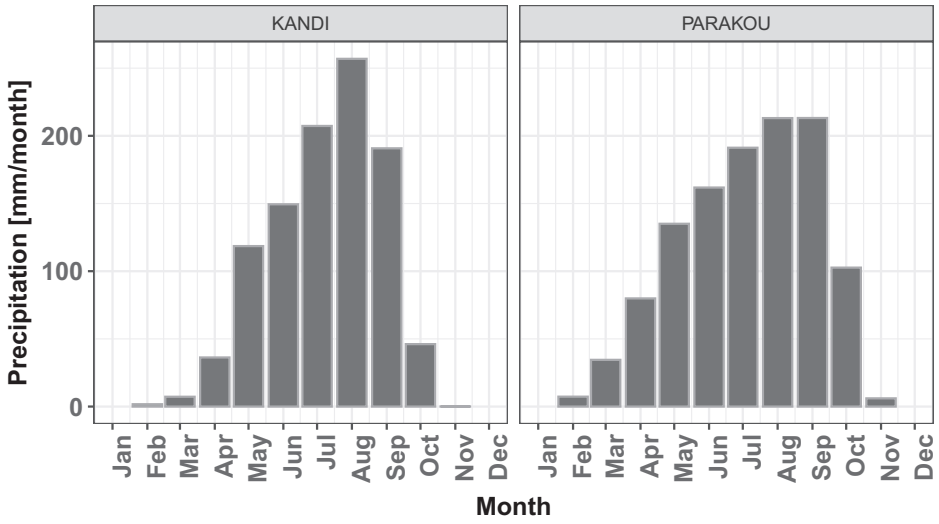

FIGURE 3 Average seasonal cycle of monthly precipitation at Kandi and Parakou rain gauges (period 1991–2020)

reference period taken into account for the observations (climatology) was 1971–2000.

2.4 | Case study area and data

Kandi and Parakou (Figure 2), two municipalities in the northern region of the Republic of Benin in West Africa, were chosen for this study. These municipalities are situated in the central part of the West African RCOF coverage area (Figure 2). The region is characterized by a plateau with an elevation ranging from 250 to 350 m. Kandi is located within the Niger River catchment area, while Parakou lies within the Oueme River catchment area. Both municipalities are home to synoptic weather stations operated by the Benin National Meteorology Agency (METEO BENIN). The climate of these areas falls under the Sudanese classification and is characterized by two distinct seasons. The rainy season typically spans from April to October, while the dry season occurs from November to March (Figure 3). The average annual rainfall in Kandi and Parakou (1991–2020) amounts to approximately 1047 and 1151 mm, respectively. Notably, the months of July, August and September (JAS) contribute to over 50% of the total annual rainfall in both municipalities. These regions are mainly engaged in agricultural activities (INSAE, 2016; Toko, 2013), with the most commonly grown crops like maize (*Zea mays* L.) and sorghum (*Sorghum*). Like most of the municipalities in Benin, the populations of Kandi and Parakou are vulnerable to interannual and intraseasonal rainfall variabilities (Boko et al., 2012), highlighting the crucial need for seasonal rainfall forecasts to drive appropriate adaptation strategies.

For this study, two climate datasets were used:

- The daily precipitation series from 1971 to 2020 for the Kandi and Parakou rain gauges from the database of METEO BENIN as shown in Figure 3.
- Seasonal climate forecast maps of cumulative rainfall from the archives of ACMAD and CRA from 1998 to 2019 as illustrated in Figure 1. These seasonal forecasts are presented in the categorical "Tercile" format.

3 | RESULTS

3.1 | Performance of SRGs in reproducing observation

The validation of rainfall occurrences is based on the analysis of the ability of SRGs to reproduce dry and wet spells statistics, as shown in Figures 4 and 5. For the JAS period (1971–2020), the average length of dry spells was 1.9 days with a standard deviation of 1.24 days for Kandi and 2.03 days with a standard deviation of 1.54 days for Parakou (Figure 4a). The maximum length of dry spells was 8 days for Kandi and 12 days for Parakou, with four dry spells lasting more than 7 days in Kandi and 18 in Parakou. On the other hand, the average length of wet spells was 2.1 days with a standard deviation of 1.65 days for Kandi and 2.28 days with a standard deviation of 1.72 days for Parakou. The maximum length of wet spells reached 23 days for Kandi and 16 days for Parakou (Figure 5a).

Figures 4a and 5a demonstrate a good agreement between the series generated by SRGs and the observations regarding mean and variance for both dry and wet spell lengths. The differences are mostly less than 0.1 days for all SRGs. The distributions of *p*-values, as shown in Figures 4b and 5b, indicate that, except for a few simulations, there was no significant difference between the generated series

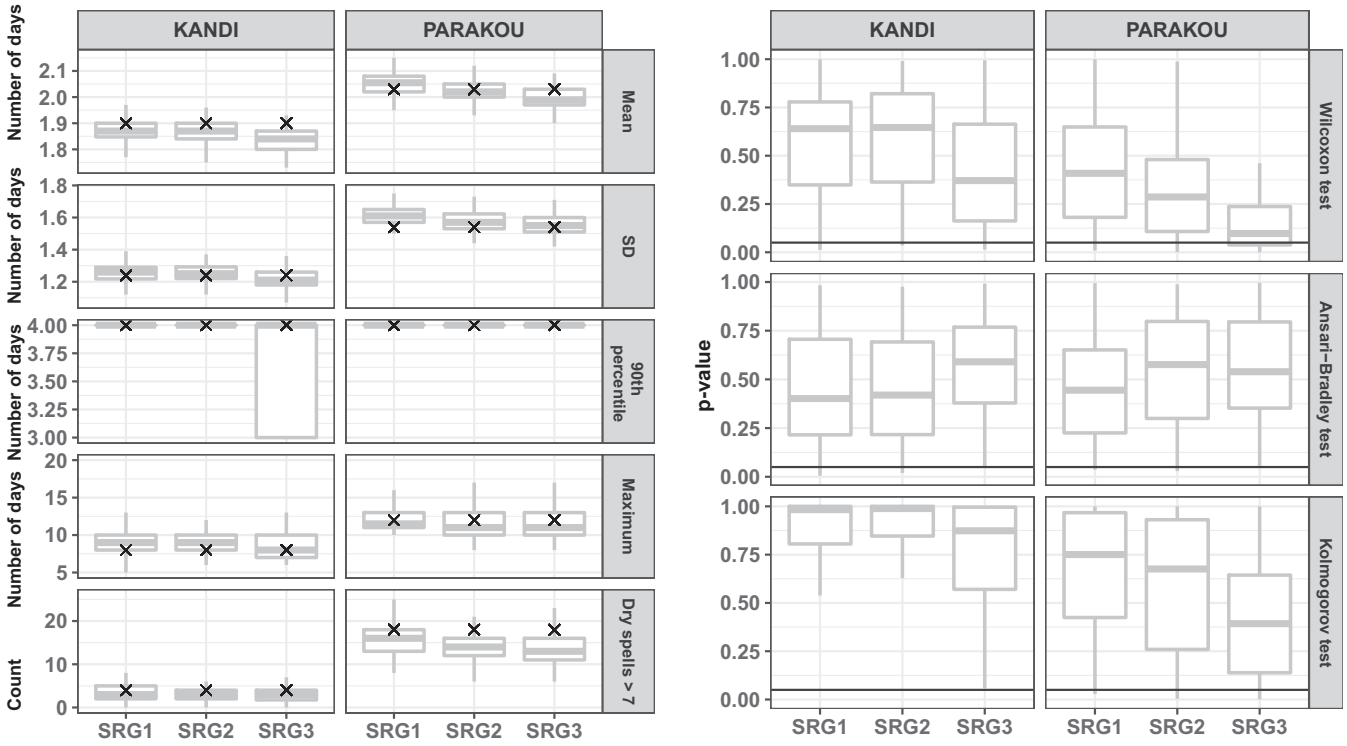

(a) Statistics on dry spells series

(b) p-value of statistical tests

FIGURE 4 Dry spell statistics (a) and *p*-value of statistical tests (b) for the July–August–September season at the Kandi and Parakou rain gauges, covering the period from 1971 to 2020 for observations (Obs) and 100 realizations of 50 seasons for SRGs. SD stands for standard deviation. The symbol **X** denotes observations, and the horizontal line indicates *p*-value = 0.05

and the observations in terms of mean (Wilcoxon test), variance (Ansari-Bradley test) and distribution (Kolmogorov test). The generated maximum values are also consistent with the observations at the Parakou station for both dry and wet spell lengths. Conversely, all SRGs underestimate the maximum wet spell lengths at the Kandi station. This station has recorded an exceptionally long wet spell of 23 days (in 1999), which is challenging to reproduce using SRGs. Nonetheless, SRGs demonstrate their effectiveness in reproducing dry spell occurrences lasting more than 7 days.

Figure 6 displays the daily rainfall statistics. Observation averages for Kandi and Parakou were 7.5 and 6.6 mm·day^{-1}, respectively, with high variability (13.4 and 14.2 mm). The highest cumulative daily rainfall was 133.8 mm in Kandi and 176 mm in Parakou (Figure 6a). Comparing the observations with the SRGs (Figure 6b), there was no significant difference in terms of averages for more than 90% of the simulations and the two stations considered. However, at the Parakou station, a significant difference was observed between the observed variance and that of the SRG1 for all the simulations. It was not the case for the SRG1 and SRG2 for more than 47% of the simulations. Considering Kandi's station, no significant difference in terms of variance was observed between the observations and SRGs for more than 60% of the simulations. The distributions of the daily rainfall from SRG2 and SRG3 were similar to the observed rainfall according to the Kolmogorov–Smirnov test for most of the simulations. The rainfall amounts simulated by SRG3 were, on average, higher than the observations and showed significant dispersion. Regarding the maximum cumulative daily rainfall, SRG2 and SRG3 were nearly identical, with SRG3 showing a lower dispersion. The PDFs of the daily rainfall on wet days (rainfall greater than 0.1) were plotted to evaluate the agreement between the simulated and observed series. SRG2's probability density curves closely matched the observations, while a slight discrepancy was observed with SRG1 and SRG3's curves (Figure S1, Supporting Information). For rainfall amounts less than 1 mm, the probability density curves of SRG1 and SRG3 were lower than the observation. The opposite was observed for rainfall amounts greater than 1 mm. The quantile–quantile diagram (Figure S2) showed that SRG2 and SRG3 accurately reproduced the observed quantiles for values less than 100 mm. However, these SRGs deviated from the observations for the extreme quantiles.

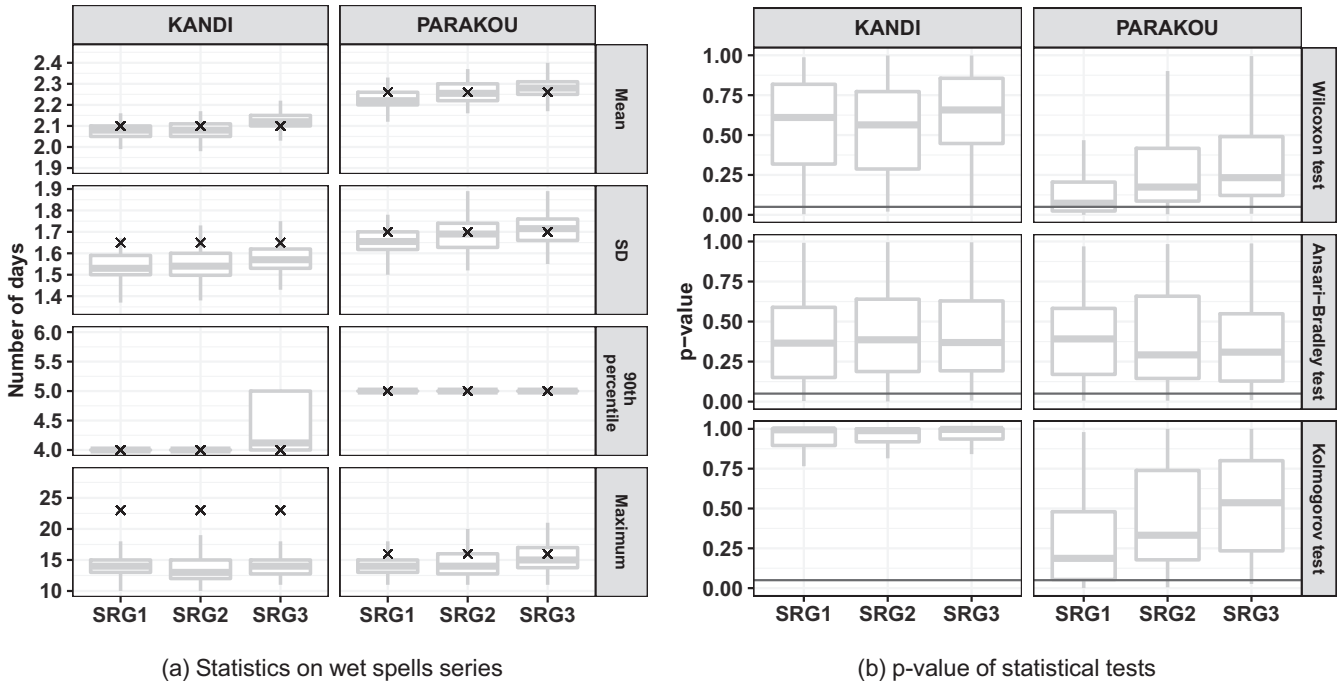

(a) Statistics on wet spells series (b) p-value of statistical tests

FIGURE 5 Wet spell statistics (a) and *p*-value of statistical tests (b) for the July–August–September season at the Kandi and Parakou rain gauges, covering the period 1971–2020 for observations (Obs) and 100 realizations of 50 seasons for SRGs. SD stands for standard deviation. The symbol **X** denotes observation, and the horizontal line indicates *p*-value = 0.05

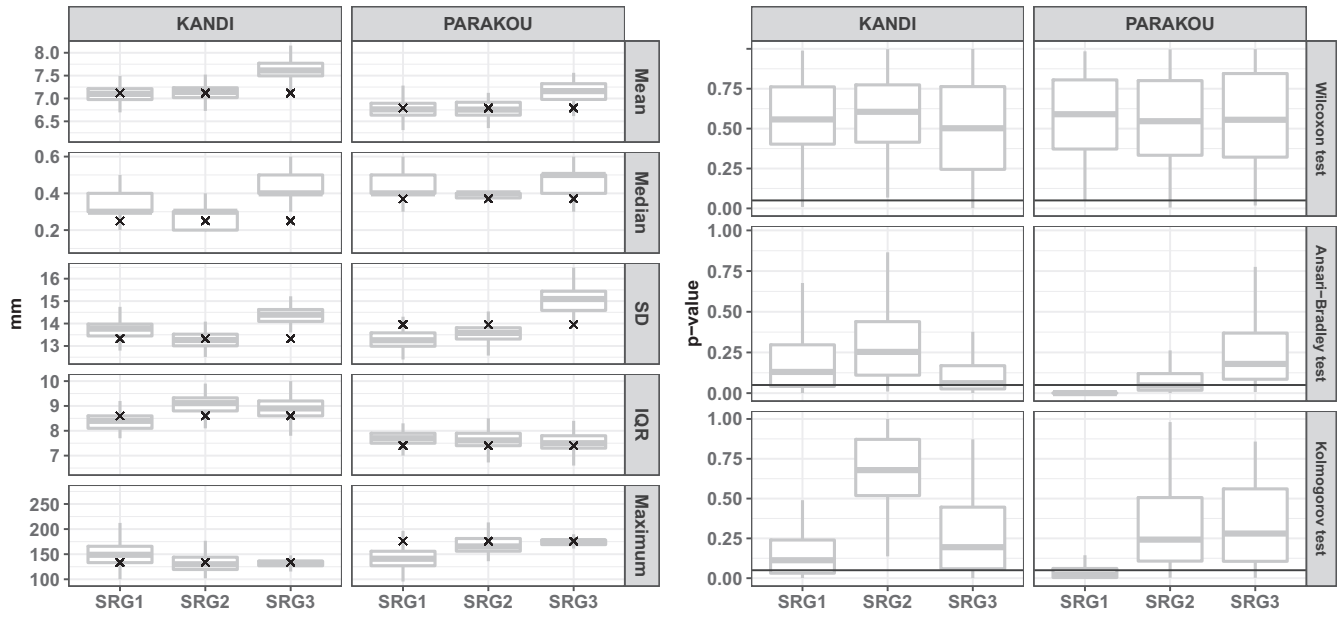

(a) Statistics on daily cumulative rainfall (b) p-value of statistical tests.

FIGURE 6 Daily rainfall statistics (a) and *p*-value of statistical tests (b) for the July–August–September season at Kandi and Parakou rain gauges, covering the period 1971–2020 for observations (Obs) and 100 realizations of 50 seasons for SRGs. SD stands for standard deviation. The symbol **X** denotes observation, and the horizontal line indicates *p*-value = 0.05

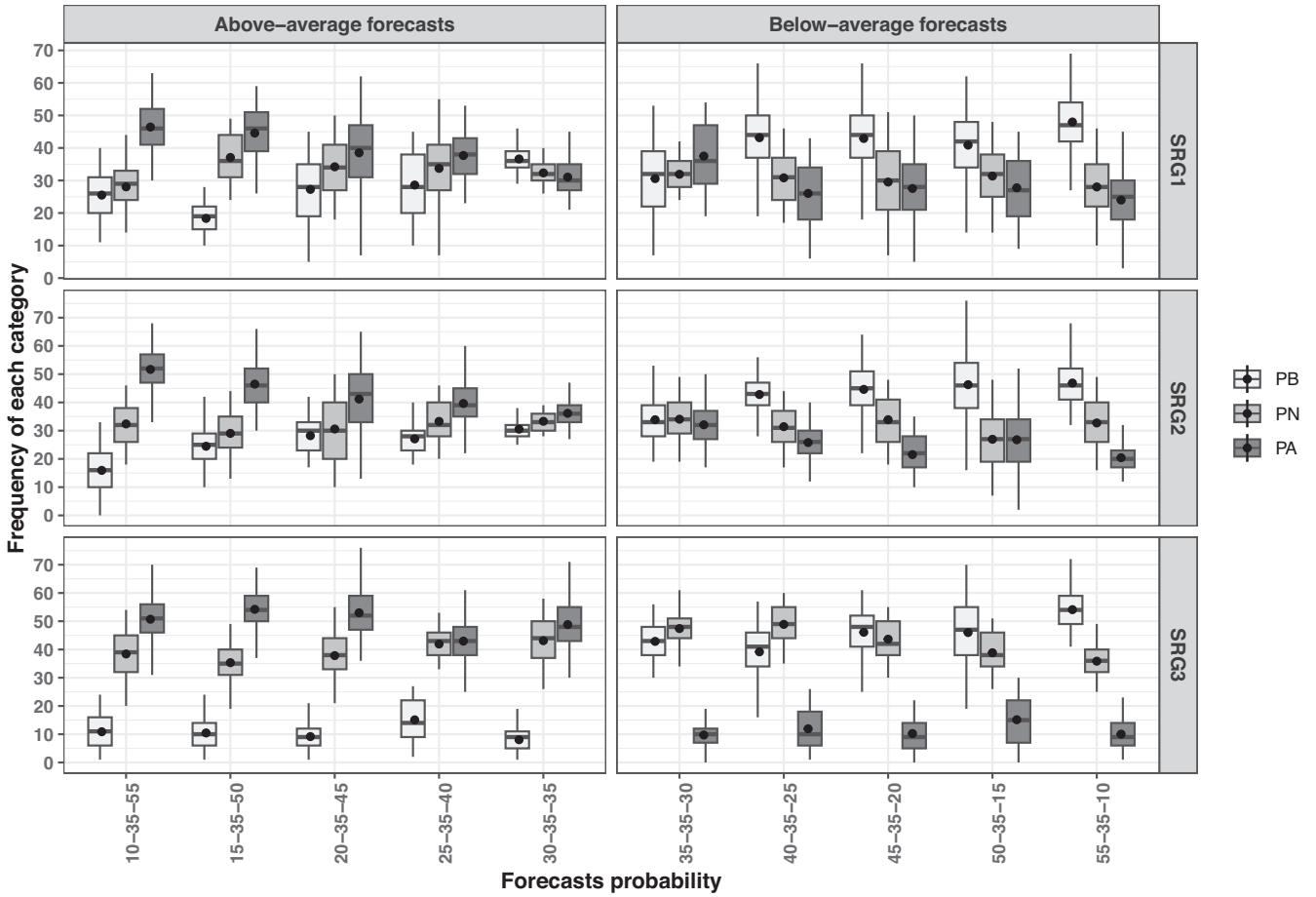

FIGURE 7 Frequencies (by conditionally generating 1000 simulations of 100 JAS daily rainy seasons for each forecast and both locations) of the below-average (PB), average (PN) and above-average (PA) categories, as functions of above-average and below-average West African RCOF seasonal rainfall forecast formats. The dots indicate the average frequencies for each category

3.2 | Analysis of disaggregated seasonal forecasts

3.2.1 | Consistency between West African RCOFs seasonal rainfall forecasts format and those obtained from disaggregated forecasts

Figures 7 and 8 display the frequencies resulting from the disaggregation of the thousand realizations for each SRG, each category of the initial forecast, and both locations. Red, green and blue dots represent the average frequency for the below-average, average and above-average categories. Tables S1 and S2 provide a concise summary of these values for a better understanding. Figure 7 predominantly shows the initial below-average and above-average categories, while Figure 8 mainly highlights the average category. Furthermore, Figure 9 illustrates the *p*-values obtained from the chi-square test for each simulation when comparing the frequencies obtained for the three categories with the categories of the initial forecasts.

The category forecasts resulting from the disaggregation of the below-average and above-average forecasts (Figure 7) maintained, to some extent, the initial signal for SRG2. This means that the distribution of PB, PN and PA is well separated when the above or below average were predominant, while it was grouped around 33% when all categories had similar probabilities (between 30% and 35%). The average frequencies after disaggregation were as follows: 15–34–51, 23–30–47, 28–32–40, 27–33–40, 31–33–36, 34–34–32, 42–32–26, 46–33–21, 48–32–31 and 46–34–20, respectively, for the 10–35–55, 15–35–50, 20–35–45, 25–35–40, 30–35–35, 35–35–30, 40–35–25, 45–35–20, 50–35–15 and 55–35–10 forecasts (Table S1). On average, SRG1 also preserved the forecast signals expressed by the probabilities of 10–35–55, 15–35–50, 20–35–45, 25–35–40, 40–35–25, 45–35–20, 50–35–15 and 55–35–15 (Figure 7), with average proportions of 25–29–46, 17–37–46, 26–34–40, 27–33–37, 42–31–27, 44–29–27, 43–31–26 and 47–29–24. Compared to SRG2, SRG1 had a wider dispersion in each category distribution. SRG3 only respected the trends of the

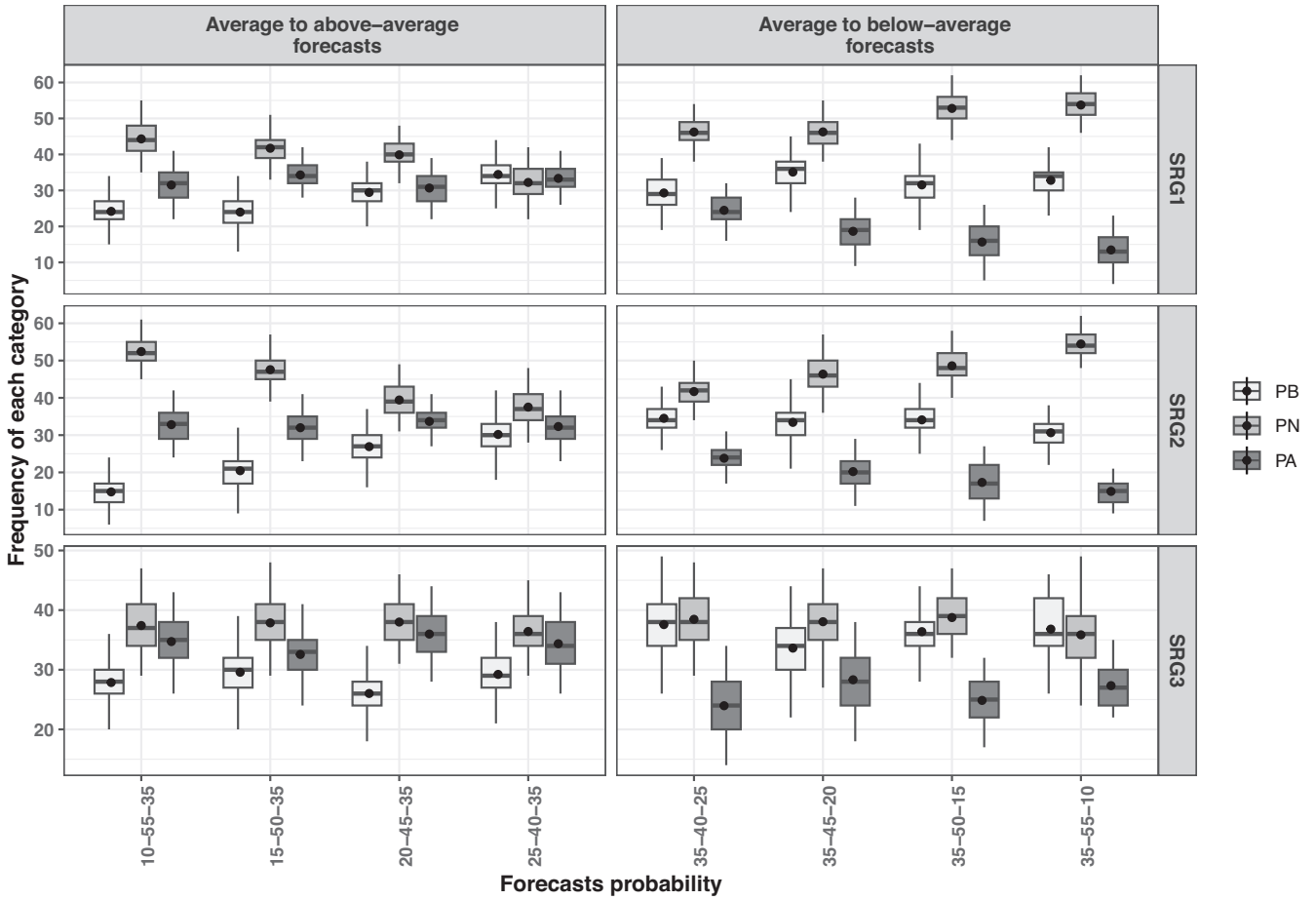

FIGURE 8 Frequencies (by conditionally generating 1000 simulations of 100 JAS daily rainy seasons for each forecast and both locations) of the below-average (PB), average (PN) and above-average (PA) categories, as functions of average West African RCOF seasonal rainfall forecast formats. The dots indicate the average frequencies for each category

initial forecasts, but there was a significant discrepancy between the categories (10–35–55, 15–35–50, 20–35–45, 50–35–15, 55–35–10).

Regarding the forecasts where the average category predominated (Figure 8 and Table S2), the frequencies obtained after disaggregation with SRG1 and SRG2 were observed to respect the trends of the initial forecasts. SRG3, on the other hand, systematically simulated 40% of the majority of the predominant average category, regardless of the initial PN value. It also exhibited a substantial dispersion compared to SRG1 and SRG2.

The *p*-values of the chi-square test in Figure 9 support these results. For SRG2, there were no significant differences between the proportions obtained after disaggregation and the categories of the initial forecasts (expected proportions) for 75% of the simulations for the initial forecasts 25–35–40, 30–35–35, 35–35–30 and 40–35–25, for more than 50% of the simulations for the 10–35–55 and 45–35–20 forecasts, and for less than 50% of the simulations for the 10–35–50, 20–35–45, 50–35–15, and 55–35–10 forecasts. For SRG1, the frequencies obtained after disaggregation are equivalent to the categories of the initial forecasts for more than 50% of the simulations for the 10–35–55, 15–35–50 and 40–35–25 forecasts and less than 50% of the simulations for the 20–35–45, 45–35–20, 50–35–15 and 55–35–10 forecasts. Globally, this is a weaker performance than SRG2 but still acceptable for the predominant average forecasts. For these simulations, it was found that SRG1 and SRG2 effectively discriminate the categories. For SRG3, there was a significant difference between the proportions after disaggregation and the categories of the initial forecasts for all simulations, except for the 40/45% of the average predominant prescribed PN values.

In summary, SRG2 outperformed both SRG1 and SRG3 in all categories. Among the three SRGs, SRG3 performed the worst. Additionally, the SRGs performed better in terms of average forecasts compared to below-average and above-average forecasts.

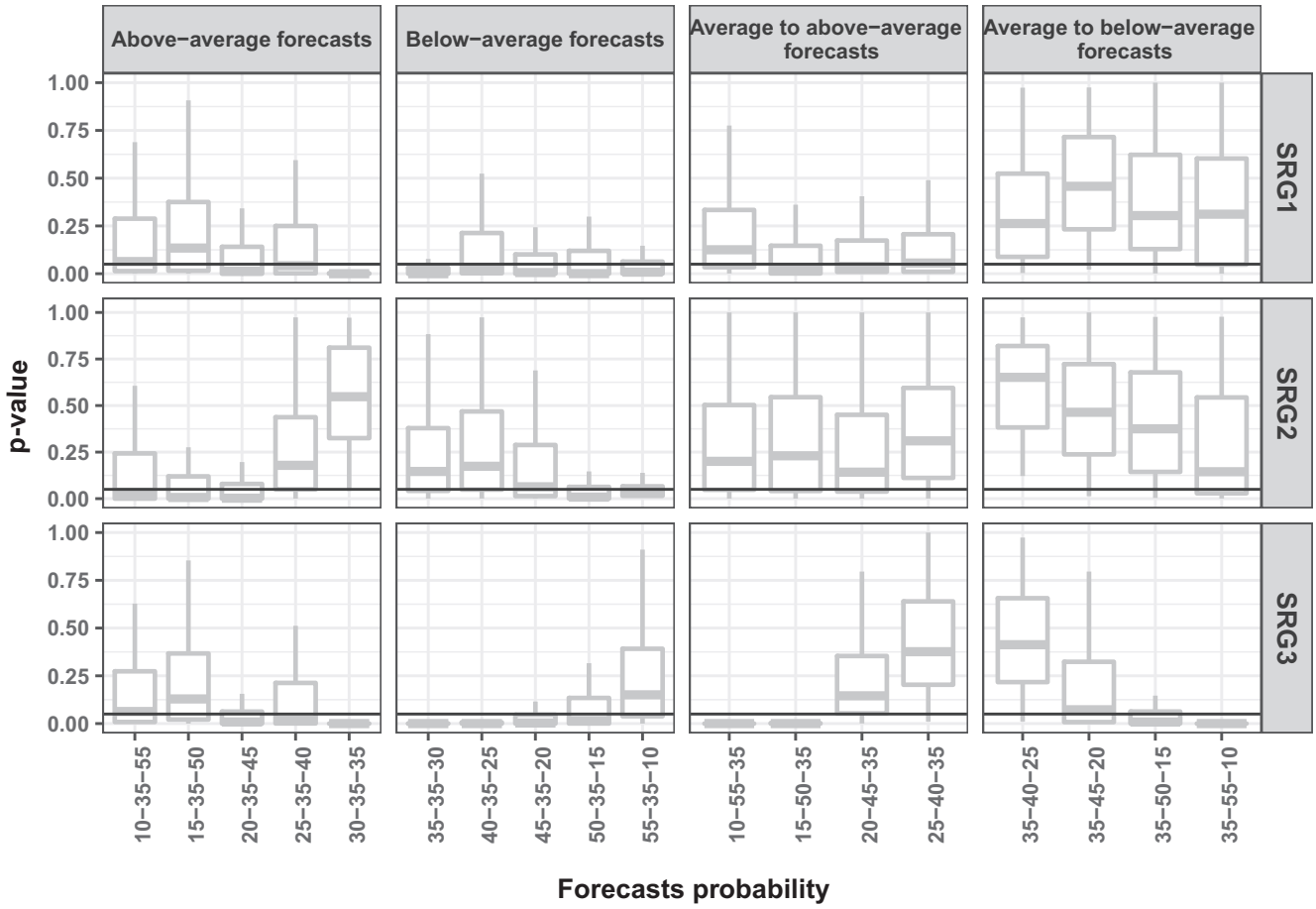

FIGURE 9 *p*-values of the chi-square goodness-of-fit test comparing the frequencies obtained (in conditionally generating 1000 simulations of 100 JAS daily rainy seasons for each forecast and station) for the three categories (below-average, average and above-average) with the categories of initial forecasts at the 5% level of significance. The horizontal line indicates *p*-value = 0.05

3.2.2 | Comparison of disaggregated forecasts to climatology

The seasonal rainfall forecasts for the Kandi area in 2003 and 2008, provided by the West African RCOF, are used as examples. These forecasts were expressed as probabilities of 15–35–50 and 20–50–30. Figures 10 and 11 display cumulative distribution function (CDF) curves representing the forecasts for above-average (15–35–50) and average (20–50–30) rainfall, respectively, for each SRG model presented in this study. These CDFs were compared with observations (reference period: 1971–2000 or climatology).

Regarding the above-average forecast (15–35–50), Figure 10 shows that seasonal rainfall amounts were most likely to be greater than the second climatological tercile (680.3 mm) for all SRGs. The occurrence probability was approximately 60% for SRG2 and SRG3 and 62% for SRG1. The cumulative seasonal JAS rainfall in 2008 aligned with the forecast made at the PRESASS forum and exceeded the climatology. The likelihood of this event based on the climatological distribution was less than 5%, compared to 20% for SRGs. Compared to the climatology, a rightward shift was observed in the CDFs of all SRGs.

For the average to above-average forecast (20–50–30), the CDFs of SRG1 and SRG2 overlapped with those of the climatology, as shown in Figure 11. The cumulative seasonal rainfall had an equal chance of occurrence for these SRGs compared to the climatology. The probability of exceeding the cumulative seasonal rainfall equal to the first tercile was more than 60% for all SRGs. This forecast corresponds to the one developed at the West African RCOF Forum in 2003, and the cumulative seasonal rainfall for that year was above-average and relatively consistent with the issued forecast.

4 | DISCUSSION

SRGs have generally shown good agreement in reproducing dry and wet spells. However, it has been found that, for some climates, first-order Markov models generate

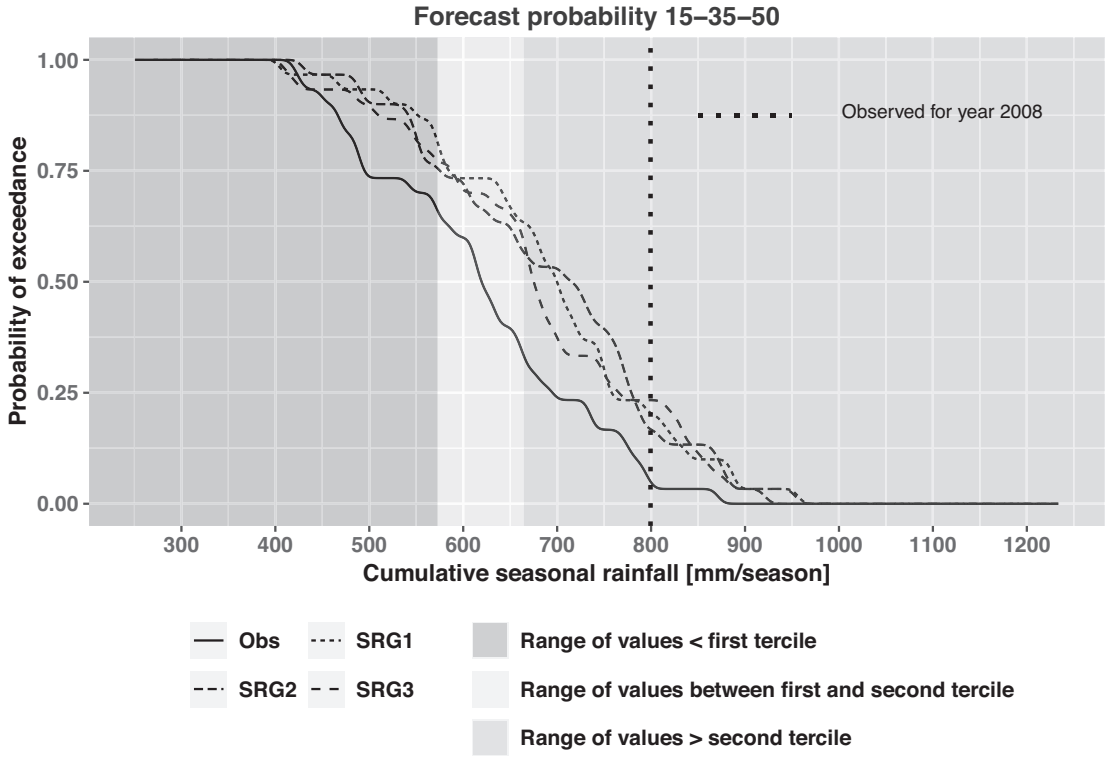

FIGURE 10 Comparison between the climatology CDF and the CDF for the seasonal amounts generated from the stochastic disaggregation models for rainfall (SRG) conditioned on the West African RCOF seasonal rainfall forecast probability (15–35–50 for the JAS season of the year 2008 at Kandi). Period 1971–2000 for climatology (Obs) and 30 disaggregated JAS seasons for SRGs. The cumulative seasonal rainfall for 2008 is shown in a dashed vertical line

synthetic precipitation series with too few long dry periods (Racsko et al., 1991; Wilks, 1999). Like other SRGs, SRG3 demonstrated good performance in reproducing maximum dry spells for the two stations, even though (Gregory et al., 1993) pointed out that a multistate Markov model requires a long historical series to estimate the parameters of the Markov chain correctly. One can conclude that the 50 years of historical data used for Kandi and Parakou stations were adequate for estimating a large number of parameters in the three-state Markov chain. SRGs also demonstrated a strong ability to reproduce the frequency of dry spells longer than 7 days, which represents a significant risk for crops during their growth phase. All SRGs replicated the mean of dry and wet spells, consistent with previous studies, particularly that of Houngninou et al. (2017), who worked in northern Benin and used a first-order Markov chain to model rainfall occurrences. However, poor reproduction of the longest wet spells was observed for Kandi station, possibly due to the exceptional nature of such an event (observed only once in the historical series). These kinds of events are difficult for the SRGs to capture. Among the three SRGs, only SRG2 could reproduce the mean, variance, maximum and quantiles of observed daily precipitation amounts. This could be related to the model used for simulating precipitation amounts in SRG2. According to Wilks and Wilby (1999), this model usually performs better than the gamma and exponential laws for the stochastic simulation of rainfall amounts. Acharya et al. (2017) also found that SRG2 is the best model for simulating precipitation in New York City.

An important aspect of the performance of SRGs conditioned on probabilities of seasonal forecasts is that the proportion of synthetic outputs in each of the three categories should correspond to the initial probabilities (Wilks, 2002). For the parametric SRGs (SRG1 and SRG2), a good agreement was found between the initial forecast categories and the proportions obtained after disaggregation. SRG2 outperformed SRG1 in this aspect. SRG2's ability to maintain the trend between the initial and disaggregated forecast categories could be due to its good performance. The semiparametric SRG (SRG3) was the worst among the SRGs. The prevalence of average years in the historical series could explain the good performance of the SRGs in the disaggregation of average categories. However, this same prevalence could negatively affect SRG3 in the above-average and below-average categories, leading to a need for a review of the resampling method used for disaggregation.

The main results of the disaggregation of the forecasts expressed as probabilities 15–35–50 and 20–50–30 showed that SRG1 and SRG2 exhibited adequate

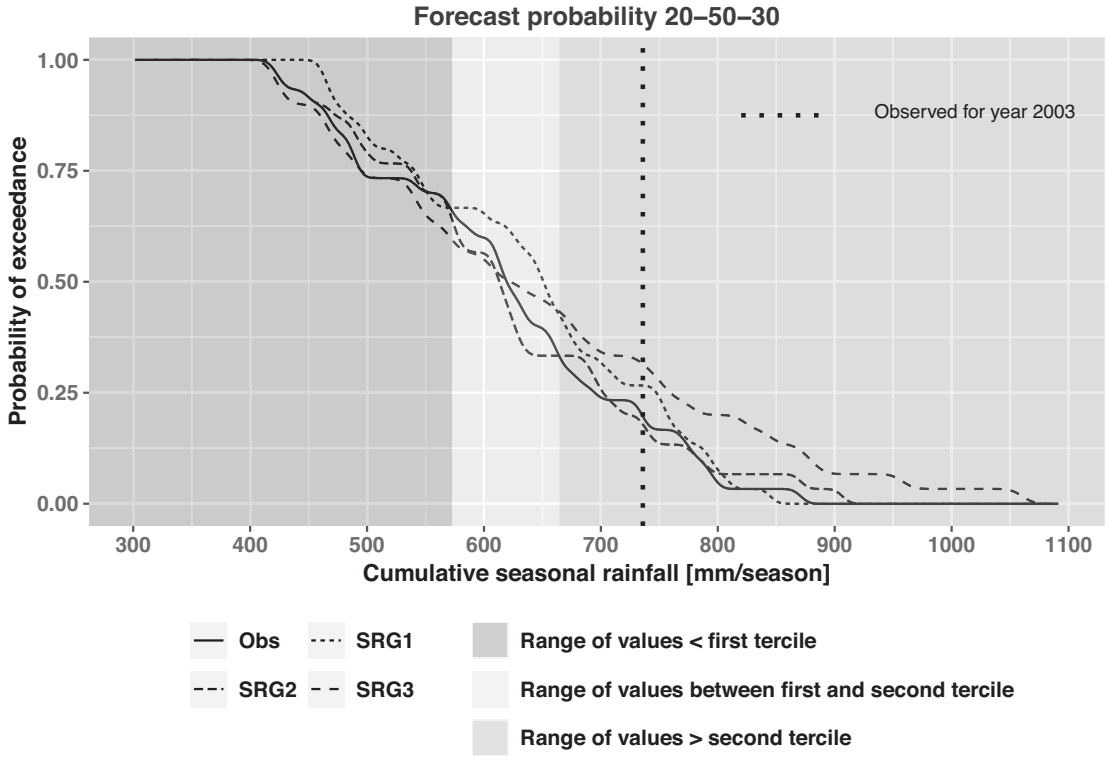

FIGURE 11 Comparison between the climatology CDF and the CDF for the seasonal amounts generated from the stochastic disaggregation models for rainfall (SRG) conditioned on the West African RCOF seasonal rainfall forecast probability (20–50–30 for the JAS season of the year 2003 at Kandi). Period 1971–2000 for climatology (Obs) and 30 disaggregated JAS seasons for SRGs. The cumulative seasonal rainfall for 2003 is shown in a dashed vertical line

behaviour compared to the climatology regarding cumulative seasonal rainfall. The CDF curves of SRGs were found to shift to the right of the climatology for above-average forecasts and interweave around the climatology for average to above-average forecasts. This behaviour was similar to that found by Apipattanavis et al. (2007, 2010), who used a semiparametric SRG in their analysis.

The main limitation of this study is the limited number of rain gauges used (only two locations in the Sudanese region) due to data availability. A larger number of rain gauge stations would be necessary to provide a more robust evaluation of the SRG methods. In particular, adding stations in the Sahelian and Guinean regions would regionally extend the usefulness of our results. Furthermore, the proposed method is built on single-site simulation and disaggregation. However, a multi-site simulation and disaggregation would better consider the spatial dependence structure of rainfall in this region and constrain the simulations more. Finally, if our method has the advantage of requiring only rainfall, using SWGs rather than SRGs could improve the relevancy of the disaggregation process by integrating, for example, other variables like air temperature, moisture, wind and so forth, for distributed applications in hydrology and agriculture. However, this is a general weakness of the West African RCOF seasonal forecasts, which have not provided forecasts for these variables.

5 | CONCLUSION

The objective of this study was to disaggregate seasonal rainfall forecasts from the West African RCOF on a daily scale. To achieve this, three SRGs were developed, and their efficiency in reproducing the main statistics of historical data was assessed. The seasonal rainfall forecasts were disaggregated by estimating the SRG parameters with a constructed historical series consistent with the forecasts. The evaluation demonstrated that the first-order two-state Markov chain, combined with a mixed exponential distribution (SRG2), performed the best in simulating rainfall occurrence and amount. This outperformed the first-order two-state Markov chain combined with a gamma distribution (SRG1) and the first-order three-state Markov chain combined with a kernel density estimation (SRG3). Regarding seasonal rainfall forecast disaggregation, the chi-square test showed that SRG2 maintained the trends of the initial forecasts and did

better than SRG1 and SRG3. The chi-square test confirmed the agreement between the initial forecasts and the frequencies obtained after disaggregation. Furthermore, the representation of forecasts disaggregated by the CDF curves revealed an appropriate shift of the curves with respect to that of the climatology. This study provides a useful guideline for producing sector-specific (hydrology, agriculture, etc.) seasonal forecasts relevant to the West Africa region. However, robust methods for constructing climatology more consistent with seasonal forecasts must be explored to improve this work. Additionally, this study only produces daily precipitation time series on a local scale, so there is a need to develop a spatial and temporal disaggregation tool for the subregion. This tool must consider other parameters, such as temperature, wind, humidity and so forth, to apply sector-specific seasonal forecasts.

AUTHOR CONTRIBUTIONS

Mandela C. M. Houngnibo: Conceptualization; data curation; methodology; visualization; writing – original draft. **Abdou Ali:** Conceptualization; methodology; writing – review and editing. **Alhassane Agali:** Supervision; writing – review and editing. **Moussa Waongo:** Validation; writing – review and editing. **Agnidé Emmanuel Lawin:** Supervision; validation; writing – review and editing. **Jean-Martial Cohard:** Validation; writing – review and editing.

ACKNOWLEDGEMENTS

The work benefited from financial support from the Accelerating Impacts of CGIAR Climate Research for Africa (AICCRA) project, funded by the International Development Association (IDA) of the World Bank. Mandela C. M. Houngnibo would like to express gratitude to Péniel Adounkpe and Vicky Boult for their technical assistance and translation support. In addition, Joseph Bessou facilitated my access the METEO BENIN data. May they be thanked.

CONFLICT OF INTEREST STATEMENT

The authors declare no conflicts of interest.

DATA AVAILABILITY STATEMENT

Scripts are available publicly on GitHub at https://github.com/hmandela/Stochastic-disaggregation-of-seasonal-forecasts. The data can be accessed upon request from METEO BENIN.

ORCID

Mandela Coovi Mahuwètin Houngnibo https://orcid.org/0000-0001-9193-4420
Agnidé Emmanuel Lawin https://orcid.org/0000-0003-4751-3439
Jean-Martial Cohard https://orcid.org/0000-0001-8418-8888

REFERENCES

Acharya, N., Frei, A., Chen, J., DeCristofaro, L. & Owens, E.M. (2017) Evaluating stochastic precipitation generators for climate change impact studies of New York City's primary water supply. *Journal of Hydrometeorology*, 18(3), 879–896.

ACMAD. (2022a) Regional climate outlook forum for the Gulf of Guinea countries. Available from: http://acmad.net/rcc/presagg.php [Accessed on 15th February 2022]

ACMAD. (2022b) Regional climate outlook forum for West Africa, Chad and Cameroon. Available from: http://acmad.net/rcc/presao.php [Accessed on 15th February 2022]

Ali, A., Amani, A., Lebel, T. & Ibrahima, S. (2006) Utilisation optimale de l'information pluviométrique des MCGA aux échelles hydrologiques au Sahel. In: *Climate variability and change: hydrological impacts*, Vol. 308. Paris: AISH, pp. 430–435.

Apipattanavis, S., Bert, F., Podestá, G. & Rajagopalan, B. (2010) Linking weather generators and crop models for assessment of climate forecast outcomes. *Agricultural and Forest Meteorology*, 150(2), 166–174. Available from: https://doi.org/10.1016/j.agrformet.2009.09.012

Apipattanavis, S., Podestá, G., Rajagopalan, B. & Katz, R. (2007) A semiparametric multivariate and multisite weather generator. *Water Resources Research*, 43(11), W11401. Available from: https://doi.org/10.1029/2006WR005714

Baigorria, G.A., Hansen, J.W., Ward, N., Jones, J.W. & O'Brien, J.J. (2008) Assessing predictability of cotton yields in the southeastern United States based on regional atmospheric circulation and surface temperatures. *Journal of Applied Meteorology and Climatology*, 47(1), 76–91.

Bliefernicht, J., Waongo, M., Salack, S., Seidel, J., Laux, P. & Kunstmann, H. (2019) Quality and value of seasonal precipitation forecasts issued by the West African regional climate outlook forum. *Journal of Applied Meteorology and Climatology*, 58(3), 621–642. Available from: https://doi.org/10.1175/jamc-d-18-0066.1

Boko, M., Kosmowski, F. & Vissin, E.W. (2012) *Les Enjeux du Changement Climatique au Bénin: Programme pour le Dialogue Politique en Afrique de l'Ouest*. Bonn: Konrad-Adenauer-Stiftung, 72 p. Available from: https://www.researchgate.net/publication/287196158_Les_enjeux_du_changement_climatique_au_Benin

Briggs, W.M. & Wilks, D.S. (1996) Extension of the climate prediction center long-lead temperature and precipitation outlooks to general weather statistics. *Journal of Climate*, 9(12), 3496–3504. Available from: https://doi.org/10.1175/1520-0442(1996)009<3496:EOTCPC>2.0.CO;2

Challinor, A.J., Slingo, J.M., Wheeler, T.R., Craufurd, P.Q. & Grimes, D.I.F. (2003) Toward a combined seasonal weather and crop productivity forecasting system: determination of the working spatial scale. *Journal of Applied Meteorology*, 42(2), 175–192. Available from: https://doi.org/10.1175/1520-0450(2003)042<0175:TACSWA>2.0.CO;2

Chidzambwa, S. & Mason, S. (2008) *Report of the evaluation of Regional Climate Outlook Forecasts for Africa during the period 1997–2007*. Niamey: ACMAD, 26 p.

Fontaine, B., Gaetani, M., Ullmann, A. & Roucou, P. (2011) Time evolution of observed July–September sea surface temperature-Sahel climate teleconnection with removed quasi-global effect (1900–2008). *Journal of Geophysical Research*, 116(D4), D04105.

Gabriel, K.R. & Neumann, J. (1962) A Markov chain model for daily rainfall occurrence at Tel Aviv. *Quarterly Journal of the Royal Meteorological Society*, 88(375), 90–95.

Ghosh, K., Singh, A., Mohanty, U., Acharya, N., Pal, R., Singh, K. et al. (2014) Development of a rice yield prediction system over Bhubaneswar, India: combination of extended range forecast and CERES-rice model. *Meteorological Applications*, 22(3), 525–533.

Gregory, J.M., Wigley, T. & Jones, P. (1993) Application of Markov models to area-average daily precipitation series and interannual variability in seasonal totals. *Climate Dynamics*, 8(6), 299–310.

Han, E. & Ines, A. (2017) Downscaling probabilistic seasonal climate forecasts for decision support in agriculture: a comparison of parametric and non-parametric approach. *Climate Risk Management*, 18, 51–65. Available from: https://doi.org/10.1016/j.crm.2017.09.003

Han, E., Ines, A. & Baethgen, W. (2017) Climate-Agriculture-Modeling and Decision Tool (CAMDT): a software framework for climate risk management in agriculture. *Environmental Modelling and Software*, 95, 102–114. Available from: https://doi.org/10.1016/j.envsoft.2017.06.024

Hansen, J.W., Mason, S.J., Sun, L. & Tall, A. (2011) Review of seasonal climate forecasting for agriculture in sub-Saharan Africa. *Experimental Agriculture*, 47(2), 205–240.

Hazen, A. (1914) Storage to be provided in impounding municipal water supply. *Transactions of the American Society of Civil Engineers*, 77(1), 1539–1640.

Houngninou, B.E., Kougbéagbédè, H., Ulrich, A.C.S. & François, G.K. (2017) Evaluation of a single-site daily precipitation generator in northwestern of Benin. *International Journal of Current Research and Academic Review*, 5(12), 1–9.

Hyndman, R.J. & Fan, Y. (1996) Sample quantiles in statistical packages. *American Statistician*, 50(4), 361–365.

Ines, A. (2013) *FResampler1: a resampling and downscaling tool for seasonal climate forecasts*. New York, NY: IRI/Columbia University.

INSAE. (2016) *Cahier des villages et quartiers de ville du département de L'Alibori*. Cotonou: Institut National de la Statistique et de l'Analyse Economique, 29 p. Available from: https://instad.bj/images/docs/insae-statistiques/enquetes-recensements/RGPH/1.RGPH_4/resultats

Jimoh, O. & Webster, P. (1996) The optimum order of a Markov chain model for daily rainfall in Nigeria. *Journal of Hydrology*, 185(1–4), 45–69. Available from: https://doi.org/10.1016/s0022-1694(96)03015-6

Katz, R.W. (1977) Precipitation as a chain-dependent process. *Journal of Applied Meteorology*, 16(7), 671–676.

Kim, Y., Rajagopalan, B. & Lee, G. (2015) Temporal statistical downscaling of precipitation and temperature forecasts using a stochastic weather generator. *Advances in Atmospheric Sciences*, 33(2), 175–183. Available from: https://doi.org/10.1007/s00376-015-5115-6

Kumar, A., Ceron, J., Coelho, C., Ferranti, L., Graham, R., Jones, D. et al. (2020) Guidance on operational practices for objective seasonal forecasting. In: *Guidance prepared under the auspices of the World Meteorological Organization Commission for Climatology (CCI) and Commission for Basic Systems (CBS)*. Geneva: WMO.

Mason, S.J., Tippett, M.K., Song, L. & Muñoz, Á.G. (2022) Climate Predictability Tool version 16.2.3. Available from: https://academiccommons.columbia.edu/doi/10.7916/d8-pmdx-bd17 [Accessed 15th February 2022]

Parhi, P., Giannini, A., Gentine, P. & Lall, U. (2016) Resolving contrasting regional rainfall responses to El Niño over tropical Africa. *Journal of Climate*, 29(4), 1461–1476.

Peleg, N., Fatichi, S., Paschalis, A., Molnar, P. & Burlando, P. (2017) An advanced stochastic weather generator for simulating 2-D high-resolution climate variables. *Journal of Advances in Modeling Earth Systems*, 9(3), 1595–1627.

Racsko, P., Szeidl, L. & Semenov, M. (1991) A serial approach to local stochastic weather models. *Ecological Modelling*, 57(1–2), 27–41.

Roudier, P., Sultan, B., Quirion, P., Baron, C., Alhassane, A., Traoré, S.B. et al. (2011) An ex-ante evaluation of the use of seasonal climate forecasts for millet growers in SW Niger. *International Journal of Climatology*, 32(5), 759–771.

Silverman, B.W. (1986) In: Cox, D.R., Hinkley, D.V., Rubin, D. & Silverman, B.W. (Eds.) *Density estimation for statistics and data analysis*. Londres: Routledge, 183 p.

Sultan, B., Barbier, B., Fortilus, J., Mbaye, S.M. & Leclerc, G. (2010) Estimating the potential economic value of seasonal forecasts in West Africa: a long-term ex-ante assessment in Senegal. *Weather Climate, and Society*, 2(1), 69–87.

Sultan, B., Roudier, P. & Quirion, P. (2013) Les bénéfices de la prévision saisonnière pour l'agriculture en Afrique de l'Ouest. *Science et Changements planétaires/Sécheresse*, 24(4), 304–313.

Toko, I. (2013) Impact des activites anthropiques sur la vegetation en region soudanienne: La Commune de Kandi au Benin. *Journal de la Recherche Scientifique de l'Université de Lomé*, 15(3), 177–188.

Wilks, D.S. (1999) Interannual variability and extreme-value characteristics of several stochastic daily precipitation models. *Agricultural and Forest Meteorology*, 93(3), 153–169.

Wilks, D.S. (2002) Realizations of daily weather in forecast seasonal climate. *Journal of Hydrometeorology*, 3(2), 195–207. Available from: https://doi.org/10.1175/1525-7541(2002)003<0195:RODWIF>2.0.CO;2

Wilks, D.S. (2011) *Statistical methods in the atmospheric sciences*, 3rd edition. Amsterdam, The Netherlands: Elsevier, 676 p.

Wilks, D.S. & Wilby, R.L. (1999) The weather generation game: a review of stochastic weather models. *Progress in Physical Geography*, 23(3), 329–357.

SUPPORTING INFORMATION

Additional supporting information can be found online in the Supporting Information section at the end of this article.

How to cite this article: Houngnibo, M. C. M., Ali, A., Agali, A., Waongo, M., Lawin, A. E., & Cohard, J.-M. (2023). Stochastic disaggregation of seasonal precipitation forecasts of the West African Regional Climate Outlook Forum. *International Journal of Climatology*, 1–17. https://doi.org/10.1002/joc.8161